17th World Conference on Earthquake Engineering, 17WCEE
Sendai, Japan - September 27th to October 2nd, 2021

USE OF NEGATIVE STIFFNESS FOR COUPLED VIBRATION CONTROL STRUCTURES: AN ANALYTICAL INVESTIGATION

S. Longjam [(1)], K. Shirai [(2)]

[(1)] *Graduate Student, Graduate School of Engineering, Hokkaido University, Japan, email: sonia.longjam.h4@elms.hokudai.ac.jp*
[(2)] *Associate Professor, Faculty of Engineering, Hokkaido University, Japan, email: shirai.kazutaka@eng.hokudai.ac.jp*

Abstract

Coupled vibration control is a promising method to mitigate earthquake response by connecting two or more vibrating structural systems to each other. A typical coupled vibration control system is formed by connecting a mainframe and a subframe with a spring element and a damping element. The control effects of coupled vibration control systems vary depending on the structural parameters, such as the mass and stiffness of the mainframe and subframe and the connecting element's stiffness and damping.

Several devices that passively produce negative stiffness have been proposed for seismic response mitigation of structures. If negative stiffness is incorporated into coupled vibration control systems as a connecting spring element, it may be possible to extend the optimal tuning conditions that are sometimes difficult with only positive or zero stiffness of the connecting element. However, research on the effectiveness of negative stiffness as a connective controller between the mainframe and subframe of coupled systems is limited.

This study aimed to understand the vibration control effects of coupled structures incorporating passive negative stiffness as the connecting spring element between the mainframe and subframe. An analytical investigation using a linear two-degree-of-freedom vibrating system model representing a simplified coupled vibration-controlled building was conducted. Based on the transfer function of the relative displacement and absolute acceleration of the model, the peak amplitude was investigated for the system with various structural parameters, such as the mass and stiffness of the mainframe and subframe, stiffness (e.g., negative stiffness) of the connection, and viscous damping of the connecting element.

From the analysis, it was found that adopting negative stiffness at the connection enabled optimal tuning for the transfer function of the mainframe, even if it was impossible to achieve only by positive or zero stiffness. When optimal tuning and optimal damping were achieved by installing negative stiffness, the peak amplitude of the transfer function of the mainframe was significantly decreased compared to that for the corresponding reference case without negative stiffness and with only a damping element.

Keywords: Negative stiffness; coupled structure; transfer function; optimal tuning; optimal damping

1. Introduction

Coupled vibration control by connecting two or more vibrating structural systems to each other is a promising approach to mitigate the seismic response and damage caused by earthquakes [1-4]. Typical coupled vibration control system models are expressed by connecting a mainframe and a subframe with a spring element and a damping element. Past research has shown that the controlling performance of coupled vibration control systems varies depending on the structural parameters, such as the mass and stiffness of the mainframe and subframe and the stiffness and damping of the connecting element [2]. Depending on the conditions, it is difficult to achieve optimal tuning that minimizes the peak amplitude of the transfer function of coupled vibration structures by using only positive or zero stiffness.

To date, several vibration control devices that passively produce negative stiffness have been proposed and developed for seismic response mitigation of buildings and civil structures [5-6]. Also, one of the authors has proposed a passive negative stiffness device comprised of curved leaf springs, which uses the reversal phenomenon of elastic snap-through buckling based on geometric nonlinearity to produce negative restoring force characteristics [7].

By incorporating negative stiffness into coupled vibration control systems as the connection spring element, an extension of the optimal tuning conditions may be possible [8]. However, there has been limited research on the effectiveness of negative stiffness as a connective controller between the mainframe and subframe of coupled systems.

This paper presents an analytical investigation on the behavior of negative stiffness incorporated into coupled vibration control structures as the connecting spring element between the mainframe and subframe. The transfer function of a basic vibrating system model representing a simplified coupled vibration control building was used to numerically investigate the effectiveness of negative stiffness with a viscous damping element combined with the connecting spring.

2. Methods

2.1 Description of coupled vibration control system

This study investigated the response control effects of a coupled vibration control system for adjacent buildings. The effectiveness of the application of negative stiffness in the connecting element was numerically examined. An analytical model was a linear two-degree-of-freedom (2DOF) system, representing a simplified coupled vibration control building model. Fig. 1 shows the 2DOF model. The mainframe and subframe are connected in the horizontal direction with a spring and a viscous damper, hereafter referred to as the connecting element. For the connecting element, negative stiffness was applied as well as positive or zero stiffness.

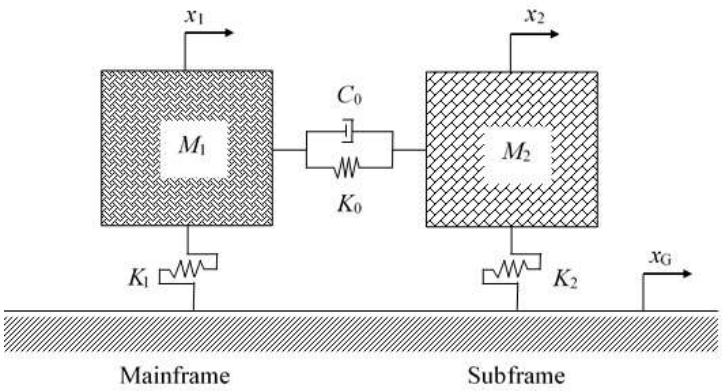

Fig. 1 – Two-degree-of-freedom coupled vibration control model

2.2 Formulation

The equations of motion of the 2DOF system can be expressed as follows:

$$M_1(\ddot{x}_1+\ddot{x}_G)+C_0(\dot{x}_1-\dot{x}_2)+K_1x_1+K_0(x_1-x_2) = 0, \tag{1}$$

$$M_2(\ddot{x}_2+\ddot{x}_G)+C_0(\dot{x}_2-\dot{x}_1)+K_2x_2+K_0(x_2-x_1) = 0, \tag{2}$$

where x_1, x_2, and x_G are the displacements of the mainframe and subframe, and ground motion, respectively, in the time domain; M_1 and M_2 are the masses of the mainframe and subframe, respectively; K_1 and K_2 are the lateral stiffnesses of the mainframe and subframe, respectively; and K_0 and C_0 are the lateral stiffness and viscous damping coefficient of the connecting element, respectively.

The equations of motion in the frequency domain can be expressed using the Laplace transform as follows:

$$M_1(s^2X_1+s^2X_G)+C_0(sX_1-sX_2)+K_1X_1+K_0(X_1-X_2) = 0, \tag{3}$$

$$M_2(s^2X_2+s^2X_G)+C_0(sX_2-sX_1)+K_2X_2+K_0(X_2-X_1) = 0, \tag{4}$$

where, X_1, X_2, and X_G are the displacements of the mainframe and subframe, and ground motion, respectively, in the frequency domain; s is the Laplace variable (= $i\omega$); i is an imaginary unit; and ω is the angular frequency.

The amplitude of the transfer function for relative displacement of the mainframe ($A_{1,\mathrm{disp}}$) and subframe ($A_{2,\mathrm{disp}}$) can be obtained as follows:

$$A_{1,\mathrm{disp}} = \frac{|X_1|}{|X_G|}, \tag{5}$$

$$A_{2,\mathrm{disp}} = \frac{|X_2|}{|X_G|}. \tag{6}$$

Also, the amplitude of the transfer function for absolute acceleration of the mainframe ($A_{1,\mathrm{acc}}$) and subframe ($A_{2,\mathrm{acc}}$) can be obtained as follows:

$$A_{1,\mathrm{acc}} = \frac{|s^2X_1+s^2X_G|}{|s^2X_G|}, \tag{7}$$

$$A_{2,\mathrm{acc}} = \frac{|s^2X_2+s^2X_G|}{|s^2X_G|}. \tag{8}$$

Because the 2DOF system has linear characteristics and a single-dashpot element, the fixed-point theory [9] in the transfer function can be adopted to determine the optimal parameters (i.e., optimal stiffness and optimal damping coefficient of the connecting element) that minimize the peak amplitude of the transfer function.

Kageyama et al. [2] proposed a theoretical formula for the optimal stiffness of the connecting element based on the fixed-point theory to achieve an optimal tuning of the 2DOF system. The optimal stiffness ($K_{0,\mathrm{opt}}$) for the displacement transfer function for the mainframe can be expressed as follows:

$$K_{0,\mathrm{opt}} = \frac{(\alpha-\mu)(-2-\mu+\alpha\mu)}{2(1+\alpha)(1+\mu)^2}K_1, \tag{9}$$

where μ (= M_2/M_1) is the mass ratio for the subframe (i.e., ratio of the mass of the subframe to that of the mainframe) and α (= K_2/K_1) is the stiffness ratio for the subframe (i.e., ratio of the lateral stiffness of the subframe to that of the mainframe).

2.3 Parameters investigated

In this study, an analytical investigation using the 2DOF system model based on the transfer function was conducted to understand the effective use of negative stiffness at the connecting element for seismic response

reduction of coupled vibration control structures. The following structural parameters for the 2DOF system were investigated:

- α: Stiffness ratio
- μ: Mass ratio

The investigated ranges for α and μ were $0 \leq \alpha \leq 2$ and $0 \leq \mu \leq 2$, respectively. Combination examples of α and μ are listed in Table 1. The parameters listed below were calculated and evaluated:

- $K_{0,opt}$: Optimal stiffness of the connecting element for optimal tuning for the displacement transfer function of the mainframe using Equation (9)
- $C_{0,opt}$: Optimal viscous damping coefficient of the connecting element for the displacement transfer function for the mainframe when $K_{0,opt}$ was given
- $h_{0,opt}$: Optimal damping ratio of $C_{0,opt}$ when $K_0 = K_{0,opt}$ [i.e., $h_{0,opt} = C_{0,opt}/(2\sqrt{M_1 K_1})$]
- $PA_{1,disp,opt}$: Peak amplitude of the displacement transfer function for the mainframe when $K_{0,opt}$ and $C_{0,opt}$ were given
- $PA_{2,disp,opt}$: Peak amplitude of the displacement transfer function for the subframe when $K_{0,opt}$ and $C_{0,opt}$ were given
- $PA_{1,acc,opt}$: Peak amplitude of the acceleration transfer function for the mainframe when $K_{0,opt}$ and $C_{0,opt}$ were given
- $PA_{2,acc,opt}$: Peak amplitude of the acceleration transfer function for the subframe when $K_{0,opt}$ and $C_{0,opt}$ were given
- $C_{0,ref}$: Reference viscous damping coefficient for the connecting portion for minimizing the peak amplitude of the displacement transfer function for the mainframe when $K_0 = 0$
- $h_{0,ref}$: Damping ratio of $C_{0,ref}$ when $K_0 = 0$ [i.e., $h_{0,ref} = C_{0,ref}/(2\sqrt{M_1 K_1})$]
- $PA_{1,disp,ref}$: Peak amplitude of the displacement transfer function for the mainframe when $K_0 = 0$ and $C_{0,ref}$ was given
- $PA_{2,disp,ref}$: Peak amplitude of the displacement transfer function for the subframe when $K_0 = 0$ and $C_{0,ref}$ was given
- $PA_{1,acc,ref}$: Peak amplitude of the acceleration transfer function for the mainframe when $K_0 = 0$ and $C_{0,ref}$ was given
- $PA_{2,acc,ref}$: Peak amplitude of the acceleration transfer function for the subframe when $K_0 = 0$ and $C_{0,ref}$ was given

3. Results

3.1 Optimal stiffness

For optimal tuning of the displacement transfer function for the mainframe, the optimal stiffness ratio ($K_{0,opt}/K_1$) was calculated against various values of α and μ using Equation (9). The obtained results of $K_{0,opt}/K_1$ are listed in Table 1. In addition, a two-dimensional (2D) contour diagram of $K_{0,opt}/K_1$ with respect to α and μ is shown in Fig. 2. These results showed that the calculated $K_{0,opt}/K_1$ varied between positive and negative values depending on parameters α and μ. Especially, in the given range of α and μ, negative stiffness (i.e., a negative value of $K_{0,opt}/K_1$) was required to achieve optimal tuning when $\mu < \alpha$.

3.2 Optimal damping

The optimal viscous damping coefficient for the connecting element ($C_{0,opt}$) that minimizes the peak amplitude of the displacement transfer function for the mainframe (when $K_0 = K_{0,opt}$) was numerically determined. The optimal damping ratio ($h_{0,opt}$) is shown in Table 2 for the cases where negative stiffness was required for $K_{0,opt}$. Also, Fig. 3 depicts a 2D contour diagram of $h_{0,opt}$ with respect to α and μ. The results showed that the optimal damping value was dependent on parameters α and μ.

For comparison, a reference viscous damping coefficient for the connecting element ($C_{0,\mathrm{ref}}$) that minimizes the peak amplitude of the displacement transfer function for the mainframe without the connecting spring element (i.e., when $K_0 = 0$) was numerically obtained. The corresponding damping ratio ($h_{0,\mathrm{ref}}$) is also shown in Table 2. Moreover, a reduction index obtained as $1-(h_{0,\mathrm{opt}}/h_{0,\mathrm{ref}})$ is listed in Table 2. The optimal damping ratio ($h_{0,\mathrm{opt}}$) when negative stiffness was applied at the connection portion (i.e., $K_0 = K_{0,\mathrm{opt}}$) was significantly reduced compared with $h_{0,\mathrm{ref}}$ without negative stiffness (i.e., $K_0 = 0$).

Table 1 – Combination examples of α and μ

α	μ	$K_{0,\mathrm{opt}}/K_1$
0.1	0.02	−0.0705
0.2	0.02	−0.1453
0.2	0.1	−0.0716
0.5	0.25	−0.1133
1.0	0.5	−0.1111
2.0	0.5	−0.1667
0.2	0.2	0
1.0	1.0	0
0.02	0.2	0.1346
0.1	0.2	0.0688
0.5	1.0	0.1042
0.5	2.0	0.1667

Table 2 – Optimal connecting stiffness ratio and optimal connecting viscous damping ratio

α	μ	$K_{0,\mathrm{opt}}/K_1$	$h_{0,\mathrm{opt}}$	$h_{0,\mathrm{ref}}$	$1-(h_{0,\mathrm{opt}}/h_{0,\mathrm{ref}})$
0.1	0.02	−0.0705	0.0063	0.0367	0.828
0.2	0.02	−0.1453	0.0135	0.0772	0.825
0.2	0.1	−0.0716	0.0149	0.0406	0.633
0.5	0.25	−0.1133	0.0421	0.0783	0.463
1.0	0.5	−0.1111	0.0750	0.1114	0.326
2.0	0.5	−0.1667	0.1696	0.2406	0.295

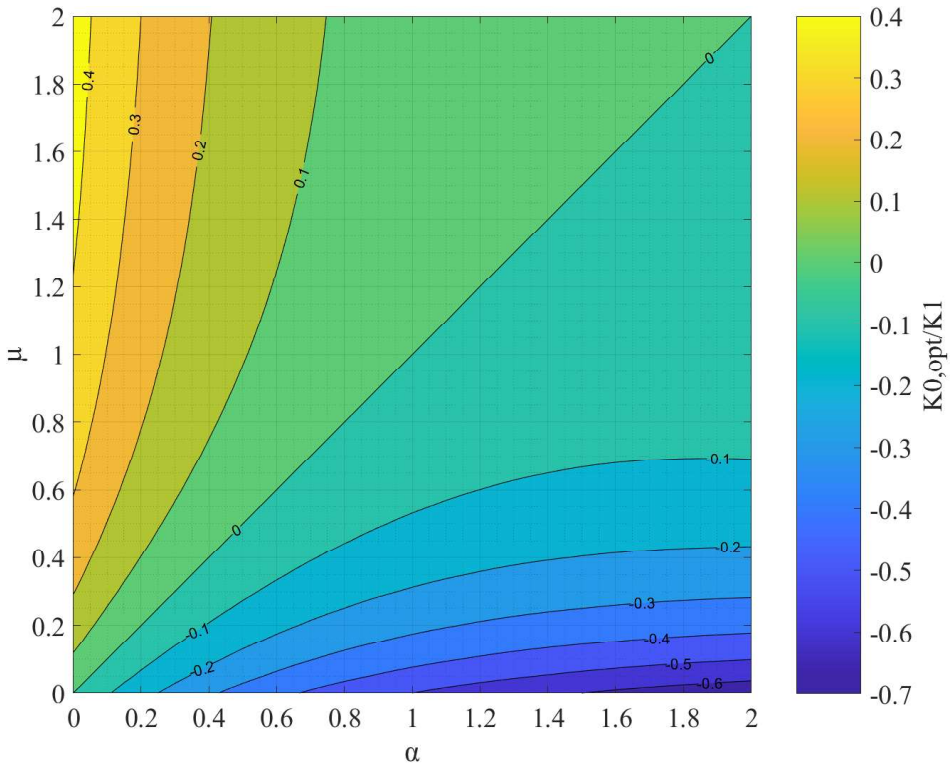

Fig. 2 – 2D contour diagram of $K_{0,\mathrm{opt}}/K_1$

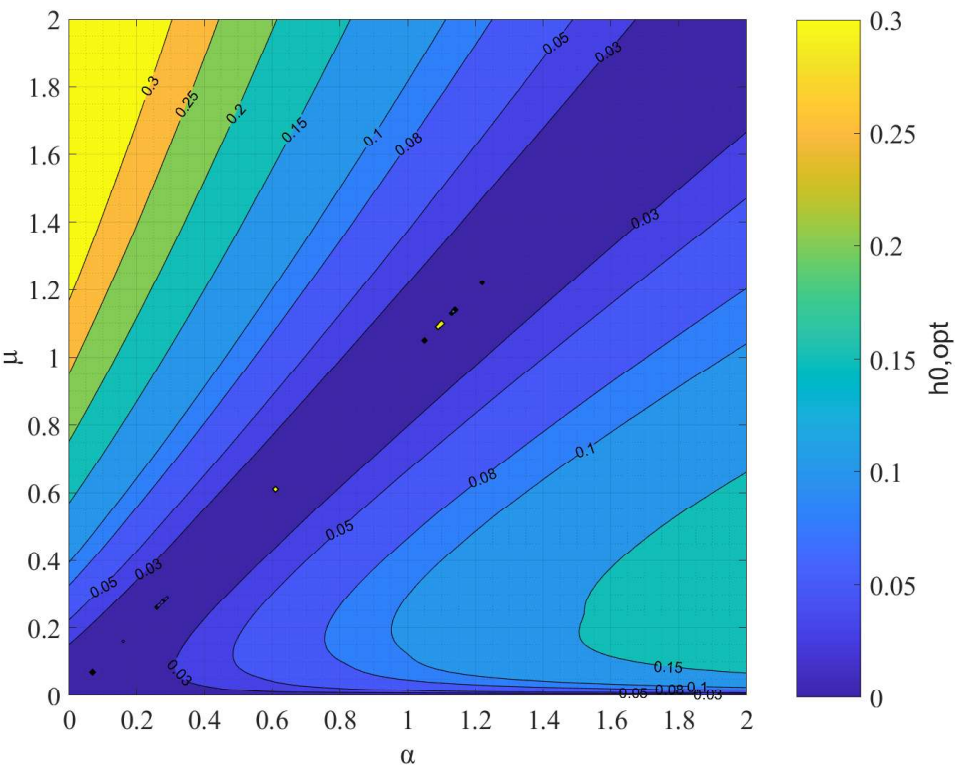

Fig. 3 – 2D contour diagram of $h_{0,\mathrm{opt}}$

3.3 Peak amplitude of the transfer function

When the optimal damping value ($C_{0,opt}$) was adopted with its corresponding optimal negative stiffness value ($K_{0,opt}$), the displacement transfer function for the mainframe was optimized. Figs. 4 and 5 show 2D contour diagrams of the peak amplitude of the displacement transfer function for the mainframe ($PA_{1,disp,opt}$) and subframe ($PA_{2,disp,opt}$), respectively, with respect to α and μ, when $K_{0,opt}$ and $C_{0,opt}$ were set for the 2DOF system. Each contour line is cut off when the value exceeds 20.

Similarly, Figs. 6 and 7 show 2D contour diagrams of the peak amplitude of the acceleration transfer function for the mainframe ($PA_{1,acc,opt}$) and subframe ($PA_{2,acc,opt}$), respectively, when $K_{0,opt}$ and $C_{0,opt}$ were used for the 2DOF system. From Fig. 4, in the given range of α and μ, the peak amplitude ($PA_{1,disp,opt}$) under the optimized condition varied depending on α and μ, and $PA_{1,disp,opt}$ generally increased as μ increased and α decreased (when $\mu < \alpha$). In Figs. 5−7, a tendency roughly similar to that shown in Fig. 4 was observed. However, comparison of the same parameters α and μ shows that the obtained peak amplitude for subframe displacement ($PA_{2,disp,opt}$) and subframe acceleration ($PA_{2,acc,opt}$) were generally larger than that for mainframe displacement ($PA_{1,disp,opt}$). In addition, the obtained peak amplitude for mainframe acceleration ($PA_{1,acc,opt}$) was generally larger than that for mainframe displacement ($PA_{1,disp,opt}$). This is because the optimization in this study was conducted by targeting the displacement transfer function for the mainframe.

Tables 3, 4, 5, and 6 show calculated values of $PA_{1,disp,opt}$, $PA_{2,disp,opt}$, $PA_{1,acc,opt}$, and $PA_{2,acc,opt}$, respectively, for the cases of α and μ (extracted from Table 1) when negative stiffness was required for optimal tuning.

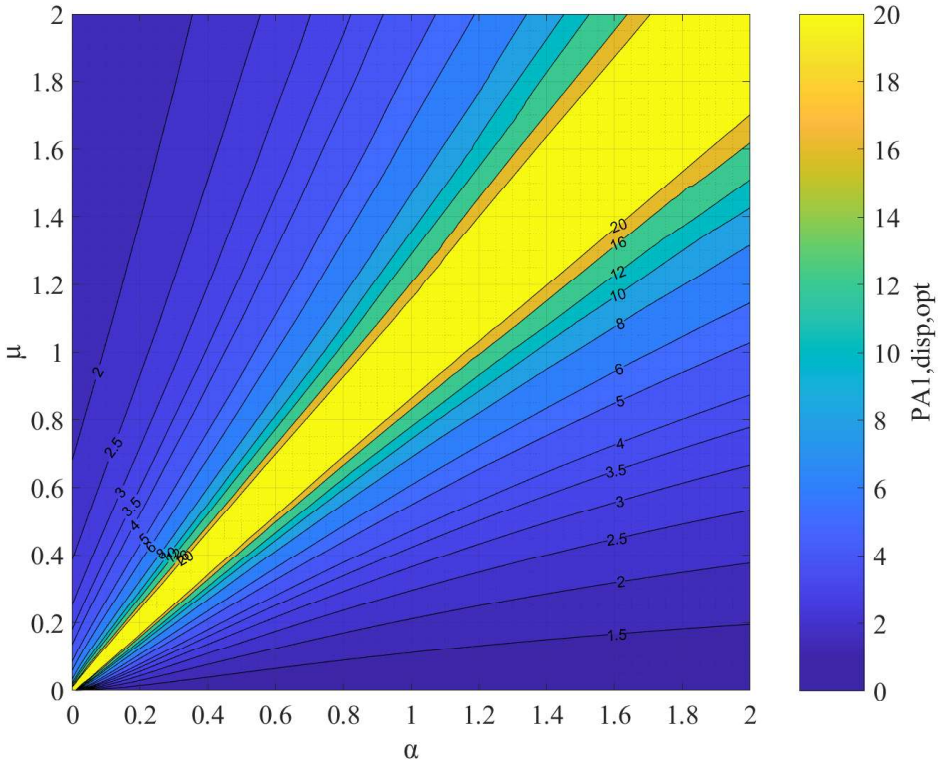

Fig. 4 – 2D contour diagram of $PA_{1,disp,opt}$

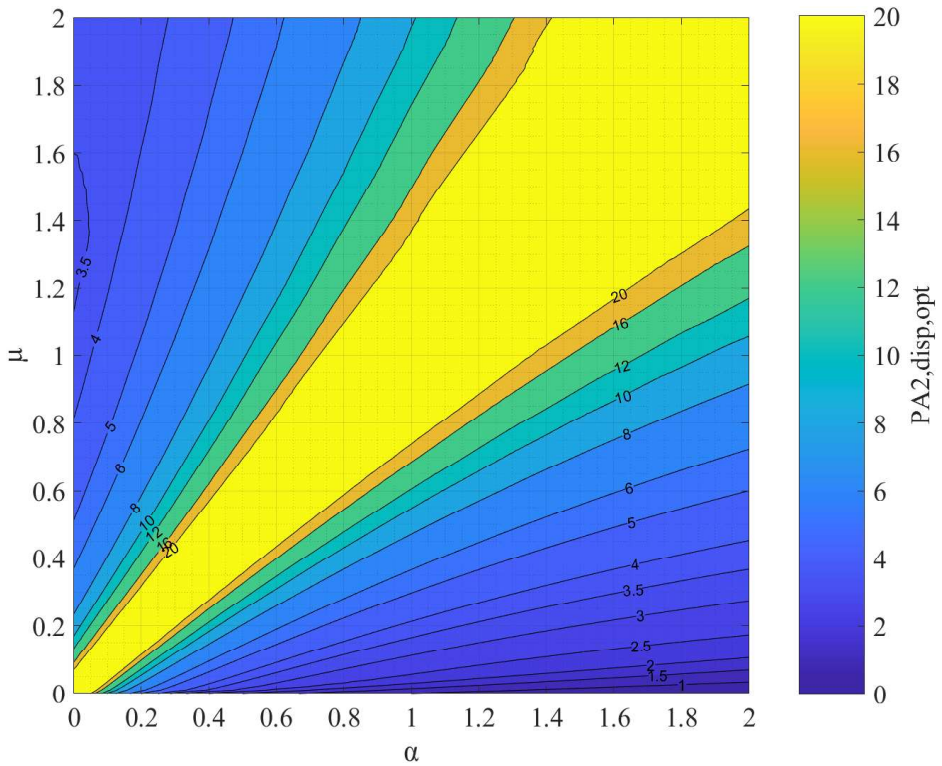

Fig. 5 – 2D contour diagram of $PA_{2,\mathrm{disp,opt}}$

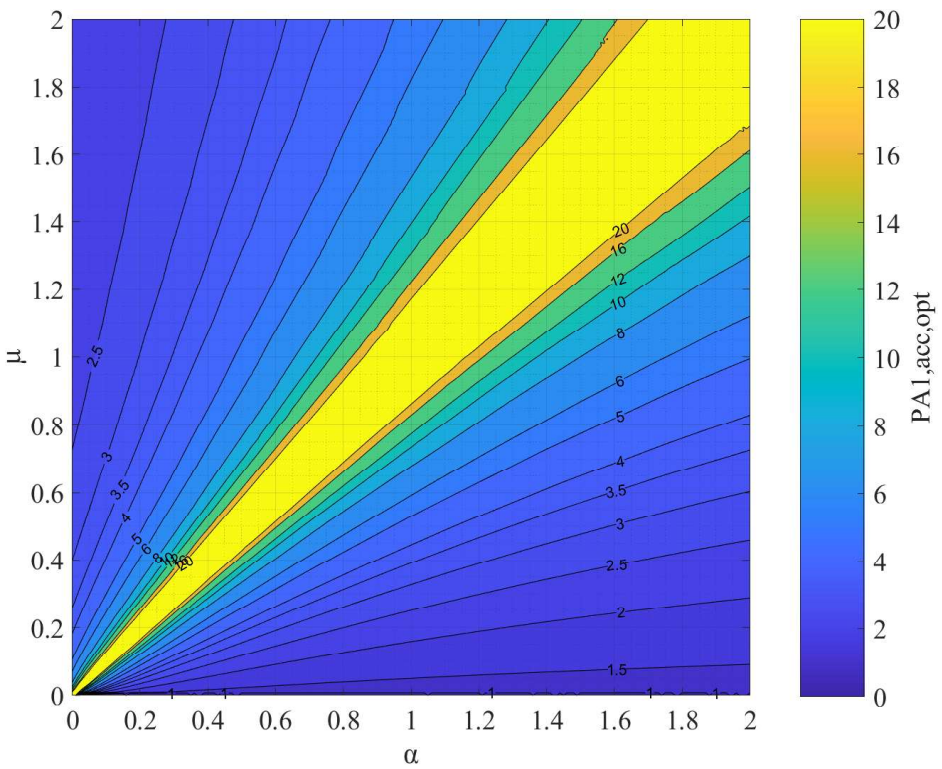

Fig. 6 – 2D contour diagram of $PA_{1,\mathrm{acc,opt}}$

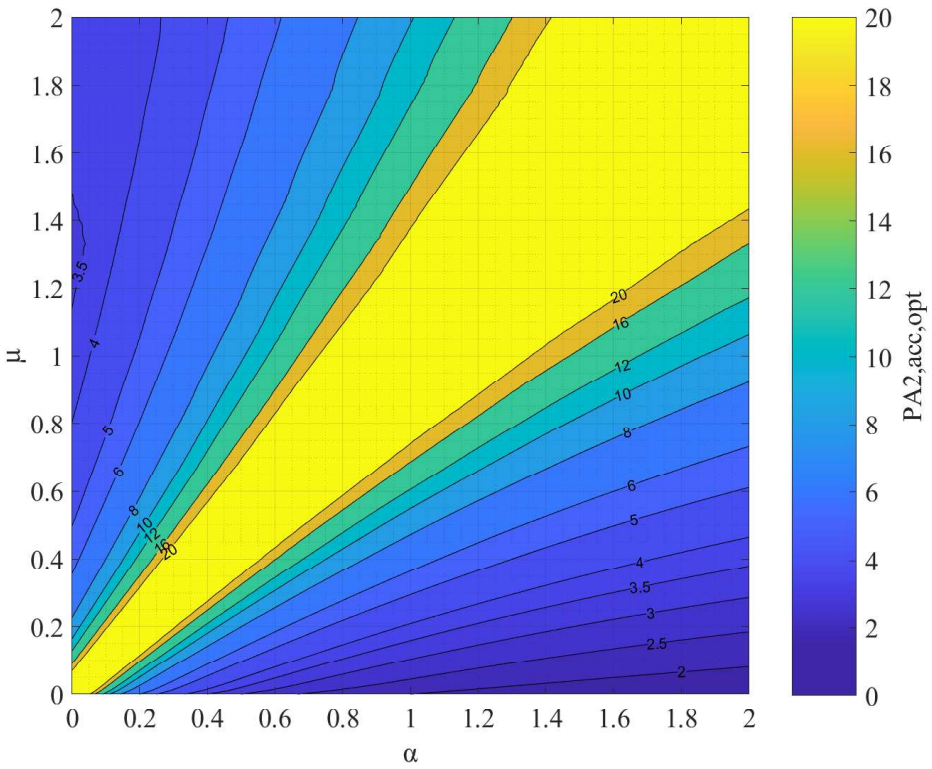

Fig. 7 – 2D contour diagram of $PA_{2,\mathrm{acc,opt}}$

3.4 Control effect achieved by negative stiffness

Table 3 gives the reference peak amplitude of the mainframe displacement transfer function ($PA_{1,\mathrm{disp,ref}}$) when $K_0 = 0$ and $C_0 = C_{0,\mathrm{ref}}$ in the 2DOF system. A reduction index obtained as $1-(PA_{1,\mathrm{disp,opt}}/PA_{1,\mathrm{disp,ref}})$ is also listed in Table 3. A significant reduction in peak amplitude was achieved by setting negative stiffness compared to the case with zero stiffness. The reduction index increased as α and μ decreased. That is, relative control effects for the mainframe achieved by negative stiffness became clearer when the stiffness and mass of the subframe were very small compared to those of the mainframe.

Table 3 – Peak amplitude of displacement transfer function for mainframe

α	μ	$PA_{1,\mathrm{disp,opt}}$	$PA_{1,\mathrm{disp,ref}}$	$1-(PA_{1,\mathrm{disp,opt}}/PA_{1,\mathrm{disp,ref}})$
0.1	0.02	2.95	26.50	0.889
0.2	0.02	1.69	12.33	0.863
0.2	0.1	5.53	23.00	0.760
0.5	0.25	4.48	11.00	0.593
1.0	0.5	4.34	7.00	0.380
2.0	0.5	2.39	3.00	0.204

Similarly, reference peak amplitudes of the transfer function for the subframe displacement ($PA_{2,\mathrm{disp,ref}}$), mainframe acceleration ($PA_{1,\mathrm{acc,ref}}$), and subframe acceleration ($PA_{2,\mathrm{acc,ref}}$) are shown in Tables 4, 5, and 6, respectively. Also, the corresponding reduction indices obtained as $1-(PA_{2,\mathrm{disp,opt}}/PA_{2,\mathrm{disp,ref}})$, $1-(PA_{1,\mathrm{acc,opt}}/PA_{1,\mathrm{acc,ref}})$, and $1-(PA_{2,\mathrm{acc,opt}}/PA_{2,\mathrm{acc,ref}})$ are given in these tables. The reduction index in Table 5 shows a tendency roughly similar to that observed in Table 3. Because the present analysis focused on optimized vibration control for the mainframe, the obtained reduction indices for the subframe [i.e., $1-(PA_{2,\mathrm{disp,opt}}/PA_{2,\mathrm{disp,ref}})$ and $1-(PA_{2,\mathrm{acc,opt}}/PA_{2,\mathrm{acc,ref}})$] were less than those for the mainframe [i.e., $1-(PA_{1,\mathrm{disp,opt}}/PA_{1,\mathrm{disp,ref}})$ and $1-(PA_{1,\mathrm{acc,opt}}/PA_{1,\mathrm{acc,ref}})$].

Table 4 – Peak amplitude of displacement transfer function for subframe

α	μ	$PA_{2,\mathrm{disp,opt}}$	$PA_{2,\mathrm{disp,ref}}$	$1-(PA_{2,\mathrm{disp,opt}}/PA_{2,\mathrm{disp,ref}})$
0.1	0.02	15.40	18.38	0.162
0.2	0.02	7.14	8.36	0.147
0.2	0.1	16.56	15.94	−0.039
0.5	0.25	10.21	7.53	−0.357
1.0	0.5	8.69	5.05	−0.721
2.0	0.5	4.30	3.05	−0.409

Table 5 – Peak amplitude of acceleration transfer function for mainframe

α	μ	$PA_{1,\mathrm{acc,opt}}$	$PA_{1,\mathrm{acc,ref}}$	$1-(PA_{1,\mathrm{acc,opt}}/PA_{1,\mathrm{acc,ref}})$
0.1	0.02	3.32	26.50	0.875
0.2	0.02	2.00	12.33	0.838
0.2	0.1	5.90	23.00	0.744
0.5	0.25	4.81	11.00	0.563
1.0	0.5	4.62	7.01	0.341
2.0	0.5	2.63	3.05	0.138

Table 6 – Peak amplitude of acceleration transfer function for subframe

α	μ	$PA_{2,\mathrm{acc,opt}}$	$PA_{2,\mathrm{acc,ref}}$	$1-(PA_{2,\mathrm{acc,opt}}/PA_{2,\mathrm{acc,ref}})$
0.1	0.02	15.91	19.10	0.167
0.2	0.02	7.61	9.09	0.162
0.2	0.1	16.84	16.66	−0.010
0.5	0.25	10.21	8.26	−0.236
1.0	0.5	8.68	5.65	−0.537
2.0	0.5	4.23	3.00	−0.410

4. Conclusions

This study conducted a numerical investigation for coupled vibration-controlled structures using negative stiffness. An analytical model of a 2DOF system connected with a spring and a dashpot was used, and the peak amplitude of the transfer function for the mainframe and subframe was evaluated.

Through the analysis, it was found that adopting negative stiffness in the connection elements enabled optimal tuning of the transfer function for the mainframe, even if it was impossible to achieve this only by positive or zero stiffness. When optimal tuning and optimal damping were obtained by incorporating negative stiffness, the peak amplitude of the transfer function for the mainframe was significantly decreased compared with that for the corresponding reference case without negative stiffness and with only the damping element.

5. References

[1] Xu YL, He Q, Ko JM (1999): Dynamic response of damper-connected adjacent buildings under earthquake excitation. *Engineering Structures*, **21** (2), 135-148.

[2] Kageyama M, Yasui Y, Seto K (2000): The principal solutions of connecting spring and damper for optimum vibration control under several criteria. *Journal of Structural and Construction Engineering*, *AIJ*, No. 529, 97-104. (in Japanese)

[3] Palacios-Quiñonero F, Rubió-Massegú J, Rossell JM, Karimi HR (2014): Vibration control for adjacent structures using local state information. *Mechatronics*, **24** (4), 336-344.

[4] Tubaldi E (2015): Dynamic behavior of adjacent buildings connected by linear viscous/viscoelastic dampers. *Structural Control and Health Monitoring*, **22** (8), 1086-1102.

[5] Iemura H, Kouchiyama O, Toyooka A, Shimoda I (2008): Development of the friction-based passive negative stiffness damper and its verification tests using shaking table. *Proceedings of the 14th World Conference on Earthquake Engineering*.

[6] Nagarajaiah S, Reinhorn AM, Constantinou MC, Taylor D, Pasala DTR, Sarlis AAS (2010): Adaptive negative stiffness: a new structural modification approach for seismic protection. *Proceedings of 5th World Conference on Structural Control and Monitoring*.

[7] Shirai K, Noro S, Walsh KK (Accepted): Shake table testing of a passive negative stiffness device with curved leaf springs for seismic response mitigation of structures. *Structural Control and Health Monitoring*.

[8] Shimizu K, Kurino H (2009): Fundamental study of structural control with negative stiffness connection. Part 1: Study of applicability of negative stiffness. *Summaries of technical papers of annual meeting, AIJ*, 453-454. (in Japanese)

[9] Den Hartog JP (1956): *Mechanical vibrations*, 4th ed. McGraw-Hill, New York.

